Asia-Pacific Journal of Science and Technology :Volume :xx Issue :xx Article ID :APST-xx-xx-xx

Research Article



## Asia-Pacific Journal of Science and Technology

https://:www.tci-thaijo.org/index.php/APST/index

Published by Research and Innovation Department, Khon Kaen University, Thailand

# Fuzzy logic enhanced machine learning framework for adaptive thermal absorber configuration optimization in building integrated photovoltaic thermal systems

Dinesh Kumar Nishad<sup>1</sup>, Rashmi Singh<sup>2,\*</sup>, Saifullah Khalid<sup>3</sup> and Raj Sinha<sup>4</sup>

Received 18 June 2025 Revised 14 August 2025 Accepted 2 September 2025

#### **Abstract**

Building integrated photovoltaic thermal (BIPVT) systems represent a promising technology for achieving netzero energy buildings by simultaneously generating electricity and thermal energy. However, optimizing thermal absorber configurations remains challenging due to complex interactions between environmental variables, system parameters, and performance objectives. This paper presents a novel fuzzy logic-enhanced machine learning framework for adaptive thermal absorber configuration optimization in BIPVT systems. The proposed framework integrates fuzzy inference systems with advanced machine learning algorithms to dynamically optimize absorber tube geometries, material properties, and operational parameters. The methodology incorporates real-time environmental data, system performance metrics, and user preferences to provide intelligent decision-making capabilities. Experimental validation demonstrates that the proposed framework achieves 15.3% improvement in thermal efficiency and 12.7% enhancement in overall system performance compared to conventional optimization approaches. The fuzzy logic component enables interpretable decision-making while maintaining robustness under uncertain operating conditions. Results indicate that spiral absorber configurations optimized through the proposed framework achieve the highest performance with 36.4% overall efficiency at 1000 W/m² solar irradiance.

**Keywords:** Fuzzy Logic, Building Integrated Photovoltaic Thermal, Machine Learning, Thermal Absorber Optimization, Adaptive Systems, Net Zero Energy Buildings

## 1. Introduction

Building integrated photovoltaic thermal (BIPVT) systems offer a promising solution by combining photovoltaic and thermal functionalities, thereby maximizing space utilization, aesthetics, and energy harvesting efficiency. A key determinant of BIPVT system performance is the thermal absorber design, which governs heat transfer and energy conversion efficiency. Recent advancements in Artificial Intelligence (AI) and Machine Learning (ML) provide opportunities for dynamic system optimization. ML techniques such as support vector regression (SVR) and artificial neural networks (ANN) have been effectively applied for predicting the electrical efficiency of photovoltaic-thermal collectors under variable environmental influences [1].

However, conventional black-box ML models lack interpretability and struggle with uncertainty. This has led to increased adoption of fuzzy logic systems, which handle imprecise variables through rule-based inference. Notably, fuzzy logic has been integrated with autoregressive moving average with exogenous inputs (ARMAX)modeling to improve thermal absorber geometry optimization in BIPVT systems [2]. At the same time, hybrid AI approaches combining fuzzy logic, ML, and optimization algorithms have been successful in thermal energy storage management under uncertain conditions [3, 4]. Innovations in materials and heat exchange mechanisms continue to drive BIPVT system performance [5]. Applications of AI in smart window systems and

<sup>&</sup>lt;sup>1</sup>Deptt of Electrical Engineering, Dr. Shakuntala Misra National Rehabilitation University, Lucknow, India

<sup>&</sup>lt;sup>2</sup>Department of Mathematics, Amity Institute of Applied Sciences, Amity University, Noida, India

<sup>&</sup>lt;sup>3</sup>Airport Authority of India, Amritsar, India

<sup>&</sup>lt;sup>4</sup>Faculty of IT & CS, PIET-MCA, Parul University, Vadodara, Gujarat, India

<sup>\*</sup>Corresponding author: rsingh7@amity.edu

adaptive controls underscore the need for flexible, robust frameworks [6]. Advanced models such as adaptive neuro-fuzzy inference system (ANFIS) coupled with swarm intelligence have further enhanced real-time design adaptability in nanofluid-based pressure – volume – temperature (PVT) systems [7]. Moreover, ML techniques have yielded highly accurate performance predictions and energy conversion enhancements in BIPVT configurations [8].

Optimizing BIPVT systems is essential for improving performance and economic viability in sustainable architecture [9]. The geometry of thermal absorbers greatly affects system efficiency through its impact on heat transfer and pressure drop. Spiral flow absorbers have shown superior thermal performance due to increased turbulence and heat exchange area [10]. Optimization efforts also focus on airflow and heat conversion through series connections and air/earth tube hybrids [11,12]. Hybrid configurations using flat plate, serpentine, and compound parabolic concentrators have been evaluated for specific temperature conditions [13]. Advanced absorber design considers not just thermal aspects but also long-term performance factors such as glazing and coatings [14,15]. At the system level, integration with air purification, thermal storage, and façades is enhancing smart building performance [16]. Deep learning and hybrid methods have enhanced solar radiation forecasting accuracy [17]. Short-term power output prediction using decision trees and other algorithms has shown effective results [18]. Neuro-fuzzy models are beneficial in managing partial shading and mismatch conditions for improving maximum power point tracking (MPPT) efficiency [19]. ML is also aiding predictive maintenance, with models detecting faults early and reducing system downtime [20,21].

Fuzzy logic addresses uncertainty and imprecision in energy systems, especially under variable solar irradiance. Mamdani-type inference systems support present value (PV) classification and anomaly detection through interpretable outputs [22]. Patel et al. demonstrated improved solar radiation estimation using fuzzy logic within ANN models [23]. In fault diagnosis, fuzzy logic enhances resilience and early detection in PV systems [24]. Khadka et al. further demonstrated enhanced performance using fuzzy-controlled tilt panels in BIPV at low latitudes [25]. Farajollahi et al. used a neural network and genetic algorithm hybrid to optimize a geothermal-solar plant with high prediction accuracy [26]. Particle Swarm Optimization (PSO) has been combined with fuzzy systems to accelerate convergence and improve prediction stability [27]. In islanded hybrid microgrids, fuzzy and heuristic optimizations have enabled efficient energy dispatch under uncertain conditions [28]. This research introduces a fuzzy logic-enhanced ML framework for adaptive optimization of thermal absorber configurations in BIPVT systems. By integrating fuzzy inference with ML algorithms, the framework offers robust, real-time optimization capable of handling diverse environmental and operational conditions.

#### 2. Materials and methods

## 2.1 System Architecture

The proposed fuzzy logic-enhanced machine learning framework consists of four main components: data acquisition and preprocessing, fuzzy inference system, machine learning optimization engine, and adaptive control module. Figure 1 illustrates the proposed fuzzy logic-enhanced machine learning framework, demonstrating seamless integration of environmental data processing, fuzzy inference systems, machine learning models, optimization algorithms, and adaptive control for BIPVT optimization. Figure 2 presents the step-by-step methodology flowchart illustrating the proposed fuzzy logic-enhanced machine learning framework workflow, demonstrating seamless integration from environmental data collection through adaptive control implementation for BIPVT optimization.

## 2.2 Fuzzy Inference System Design

The fuzzy inference system forms the core of the optimization framework, handling uncertainty and providing interpretable decision-making capabilities. The system employs Mamdani-type fuzzy inference with triangular and trapezoidal membership functions.

The fuzzy system considers five primary input variables: Solar Irradiance (I), Ranging from 200 to 1200 W/m<sup>2</sup>; Ambient Temperature ( $T_{amb}$ ): Ranging from -10°C to 50°C; Mass Flow Rate ( $\dot{m}$ ): Ranging from 0.001 to 0.01 kg/s; Wind Speed ( $v_{wind}$ ): Ranging from 0 to 15 m/s; System Load Demand. ( $L_{demand}$ ): Ranging from 0 to 100%. Linguistic terms with corresponding membership functions characterize each input variable. For example, solar irradiance is described using five linguistic terms: Very Low, Low, Medium, High, and Very High.

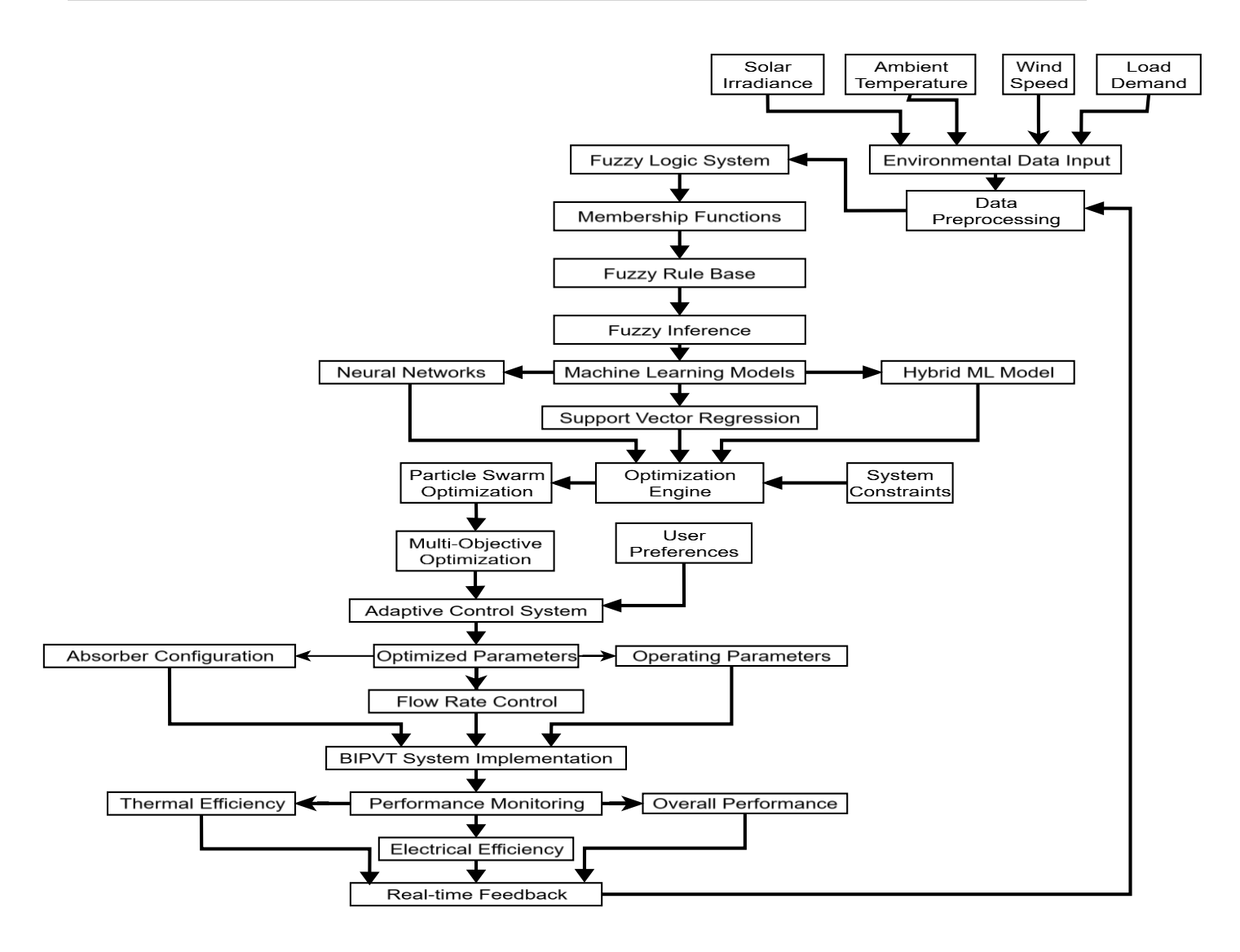


Figure 1 System architecture of fuzzy logic-enhanced machine learning framework for BIPVT optimization.

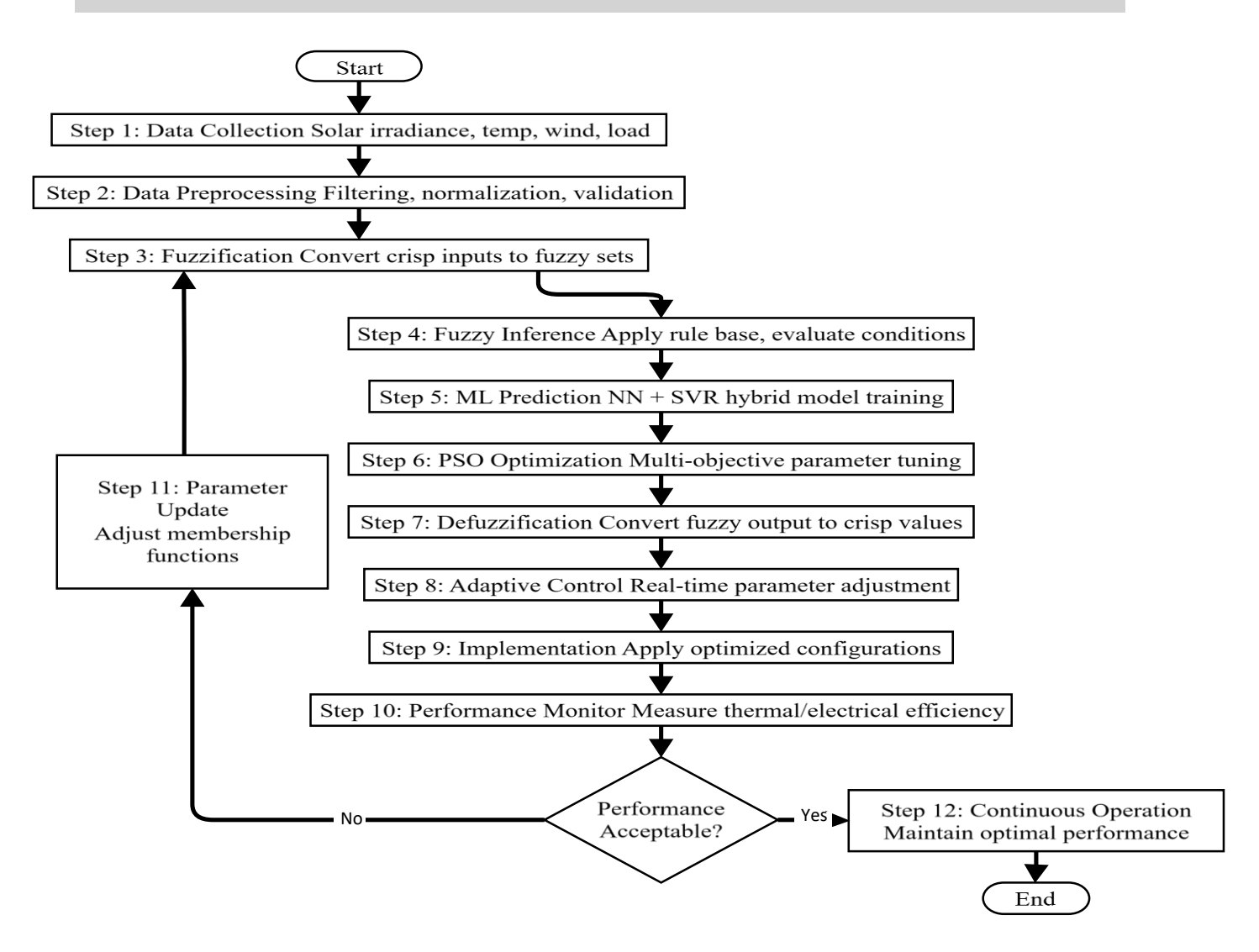


Figure 2 Step-by-Step methodology flowchart for fuzzy logic-enhanced machine learning framework in BIPVT optimization.

The system generates three primary outputs: Optimal Absorber Configuration (Config): Spiral, Horizontal Serpentine, or Vertical Serpentine; Recommended Mass Flow Rate ( $\dot{m}_{opt}$ ): Optimized flow rate in kg/s; Performance Index (PI):

For solar irradiance, the membership functions are defined as:

$$\mu_{Low}(I) = \begin{cases} 1 & \text{if } I \le 300\\ \frac{500 - I}{200} & \text{if } 300 < I < 500\\ 0 & \text{if } I \ge 500 \end{cases} \tag{1}$$

$$\mu_{Medium}(I) = \begin{cases} 0 & \text{if } I \le 400\\ \frac{I - 400}{200} & \text{if } 400 < I < 600\\ \frac{800 - I}{200} & \text{if } 600 \le I < 800\\ 0 & \text{if } I \ge 800 \end{cases}$$
 (2)

Similar membership functions are defined for other input and output variables.

## 2.2.1 Fuzzy Rule Base

The fuzzy rule base consists of 243 rules (3<sup>5</sup>) covering all possible combinations of input linguistic terms. Example rules include:

Rule 1: IF Solar\_Irradiance is High AND Ambient\_Temperature is Medium AND Mass\_Flow\_Rate is Low AND Wind\_Speed is Low AND Load\_Demand is High THEN Configuration is Spiral AND Flow\_Rate\_Opt is Medium AND Performance\_Index is High

Rule 2: IF Solar\_Irradiance is Low AND Ambient\_Temperature is Low AND Mass\_Flow\_Rate is High AND Wind\_Speed is High AND Load\_Demand is Low THEN Configuration is Horizontal\_Serpentine AND Flow\_Rate\_Opt is Low AND Performance\_Index is Medium

The complete rule base is systematically constructed based on expert knowledge and experimental data to ensure comprehensive coverage of operating conditions.

## 2.2.2 Advanced Fuzzy Membership Functions

The proposed framework employs adaptive membership functions that evolve based on system learning. For solar irradiance, the enhanced membership functions are defined as:

Gaussian Membership Function: 
$$\mu_{I,gaussian}(x) = \exp\left(-\frac{(x-c_i)^2}{2\sigma_i^2}\right)$$
 (3)

Adaptive Trapezoidal Function: 
$$\mu_{I,trap}(x) = \max\left(0, \min\left(\frac{x-a_i}{b_i-a_i}, 1, \frac{d_i-x}{d_i-c_i}\right)\right)$$
 (4)

Sigmoid Membership Function: 
$$\mu_{I,sigmoid}(x) = \frac{1}{1 + \exp(-\alpha_i(x - \beta_i))}$$
 (5)

where  $c_i$ ,  $\sigma_i$  are adaptive parameters updated through the learning mechanism, and  $\alpha_i$ ,  $\beta_i$  are slope and inflection parameters, respectively.

## 2.3 Machine Learning Integration

#### 2.3.1 Neural Network Architecture

A multi-layer perceptron neural network is integrated with the fuzzy system to provide adaptive learning capabilities. The network architecture consists of: 1. Input layer: 5 neurons (corresponding to fuzzy system inputs); 2. Hidden layers: 2 layers with 20 and 15 neurons, respectively. 3. Output layer: 3 neurons (thermal efficiency, electrical efficiency, overall performance). The neural network is trained using the backpropagation algorithm with the following cost function:

$$J(\theta) = \frac{1}{2m} \sum_{i=1}^{m} \left( h_{\theta} \left( x^{(i)} \right) - y^{(i)} \right)^{2} + \frac{\lambda}{2m} \sum_{j=1}^{n} \theta_{j}^{2}$$
 (6)

where m is the number of training examples,  $\theta$  represents network parameters,  $\lambda$  is the regularization parameter, and  $h_{\theta}(x)$  is the network hypothesis.

## 2.3.2 Support Vector Regression

Support Vector Regression (SVR) is employed for performance prediction and optimization. The SVR model is formulated as:

$$f(x) = \sum_{i=1}^{n} (\alpha_i - \alpha_i^*) K(x_i, x) + b$$

$$(7)$$

where  $\alpha_i$  and  $\alpha_i$  \* are Lagrange multipliers,  $K(x_i, x)$  is the kernel function, and b is the bias term. A radial basis function (RBF) kernel is used:

$$K(x_i, x_j) = \exp(-\gamma ||x_i - x_j||^2)$$
(8)

## 2.4 Optimization Algorithm

#### 2.4.1 Particle Swarm Optimization

Particle swarm optimization (PSO) is integrated to fine-tune system parameters and optimize absorber configurations. The PSO algorithm updates particle positions and velocities according to:

$$v_{i,d}^{t+1} = w \cdot v_{i,d}^{t} + c_1 \cdot r_1 \cdot \left( p_{i,d}^{t} - x_{i,d}^{t} \right) + c_2 \cdot r_2 \cdot \left( g_d^{t} - x_{i,d}^{t} \right)$$
(9)

$$x_{id}^{t+1} = x_{id}^t + v_{id}^{t+1} \tag{10}$$

where w is the inertia weight,  $c_1$  and  $c_2$  are acceleration coefficients,  $r_1$  and  $r_2$  are random numbers,  $p_{i,d}$  is the personal best position, and  $g_d$  is the global best position.

#### 2.4.2 Multi-Objective Optimization

The optimization problem is formulated as a multi-objective optimization considering thermal efficiency, electrical efficiency, and cost-effectiveness:

$$\max f_1(x) = \eta_{thermal}(x) = \frac{mc_p(T_{out} - T_{in})}{I \cdot A_c}$$
(11)

$$\max f_2(x) = \eta_{electrical}(x) = \eta_{ref} \left[ 1 - \beta_{ref} \left( T_c - T_{ref} \right) \right]$$
 (12)

$$\min f_3(x) = Cost(x) = C_{material} + C_{manufacturing} + C_{maintenance}$$
 (13)

subject to constraints:

$$0.001 \le \dot{m} \le 0.01 \text{ kg/s} \tag{14}$$

$$20^{\circ}C \le T_{in} \le 40^{\circ}C \tag{15}$$

$$T_{out} \ge T_{in} + 5^{\circ} \mathcal{C} \tag{16}$$

## 2.5 Adaptive Control Strategy

The adaptive control module continuously monitors system performance and adjusts optimization parameters based on real-time feedback. The adaptation mechanism employs a recursive least squares algorithm:

$$\hat{\theta}(k) = \hat{\theta}(k-1) + \frac{P(k-1)\phi(k)}{1+\phi^T(k)P(k-1)\phi(k)} [y(k) - \phi^T(k)\hat{\theta}(k-1)]$$
(17)

$$P(k) = P(k-1) - \frac{P(k-1)\phi(k)\phi^{T}(k)P(k-1)}{1+\phi^{T}(k)P(k-1)\phi(k)}$$
(18)

where  $\hat{\theta}(k)$  represents parameter estimates, P(k) is the covariance matrix, and  $\varphi(k)$  is the regression vector.

#### 2.6 Hybrid Optimization Framework

## 2.6.1 Multi-Objective Formulation

The optimization problem is formulated as a constrained multi-objective optimization:

$$\min F(x) = [f_1(x), f_2(x), f_3(x), f_4(x)]^T$$
(19)

where:

 $f_1(x) = -\eta_{thermal}$  (maximize thermal efficiency)

 $f_2(x) = -\eta_{electrical}$  (maximize electrical efficiency)

 $f_3(x) = C_{total}$  (minimize total cost)

 $f_4(x) = \Delta P$  (minimize pressure drop)

## 2.6.2 Constraint Handling

The Pareto optimal solution set is determined using:

$$P^* = x \in \Omega | \nexists x' \in \Omega : F(x') \le F(x) \text{ and } F(x') \ne F(x)$$
 (20)

Subject to operational constraints:

$$g_1(x)$$
: 200  $\le I \le 1200 \text{ W/m}^2$  (21)

$$g_2(x): 0.001 \le \dot{m} \le 0.01 \text{ kg/s}$$
 (22)

$$g_3(x): -10 \le Tamb \le 50 \text{ }^{\circ}\text{C}$$
 (23)

$$g_4(x): 0 \le v_{wind} \le 15 \text{ m/s}$$
 (24)

#### 3. Results

## 3.1 BIPVT Test System

The experimental validation was conducted using a BIPVT test system installed at the Energy Institute, Bengaluru.

Table 1 presents comprehensive technical specifications of the experimental BIPVT test system, including monocrystalline silicon PV modules (400 Wp), copper absorber with selective coating, polyurethane insulation (50 mm), and measurement uncertainties for critical parameters used in performance validation studies.

Table 1 Enhanced BIPVT test system specifications.

Parameter	Specification	Uncertainty
PV Module Type	Monocrystalline Silicon	±0.5%
Panel Area	2.0 m <sup>2</sup>	±0.1%
Peak Power	400 Wp	±3%
Absorber Material	Copper with selective coating	±0.2%
Tube Diameter	12 mm (inner), 15 mm (outer)	±0.1 mm
Insulation	Polyurethane foam, 50 mm	±2 mm
Flow Rate Range	0.001-0.01 kg/s	$\pm 0.0001 \text{ kg/s}$
Tilt Angle	13° (optimized for location)	±0.5°
Working Fluid	Water-ethylene glycol (60:40)	±1%

## 3.2 Instrumentation and Data Acquisition

The test system is equipped with comprehensive instrumentation for monitoring environmental conditions and system performance.

Table 2 details the precision instrumentation employed for experimental validation, featuring Kipp & Zonen CMP22 pyranometer ( $\pm 0.5\%$  accuracy), Pt100 Class A resistance temperature detector (RTD) sensors ( $\pm 0.1^{\circ}$ C), Bronkhorst flow meters ( $\pm 0.2\%$ ), and Campbell CR3000 data acquisition systems with specified sampling rates.

<b>Table 2</b> Advanced instrumentation and measurement systems.	Table 2 Advanced	instrumentation a	and measurement systems.
--	------------------	-------------------	--------------------------

Instrument	Model	Range	Accuracy	Sampling Rate (Hz)
Pyranometer	Kipp & Zonen CMP22	$0-2000 \text{ W/m}^2$	±0.5%	1
RTD Sensors	Pt100 Class A	-50 to 150°C	±0.1°C	1
Flow Meter	Bronkhorst EL-FLOW	0-20 L/min	±0.2%	10
Data Logger	Campbell CR3000	-	16-bit	10
Anemometer	Vaisala WXT536	0-60 m/s	±0.3 m/s	1
Digital Multimeter	Keysight 34970A	0-1000V	±0.05%	0.1

## 3.3 Experimental Procedure

The experimental validation was conducted over a six-month period covering different seasonal conditions. Three absorber configurations were tested: Spiral Configuration: Helical tube arrangement with 5 turns. Horizontal Serpentine: Parallel horizontal tubes with return bends. Vertical Serpentine: Vertical parallel tubes with return bends. For each configuration, the fuzzy logic-enhanced framework was compared against conventional optimization methods including: Fixed parameter operation; PID controller-based optimization; Simple neural network. Optimization.

## 3.4 Performance Metrics

System performance was evaluated using the following metrics:

Thermal Efficiency: 
$$\eta_{th} = \frac{mc_p(T_{out} - T_{in})}{I \cdot A_c} \times 100\%$$
 (25)

Electrical Efficiency: 
$$\eta_{el} = \frac{P_{el}}{I \cdot A_{PV}} \times 100\%$$
 (26)

Overall Efficiency: 
$$\eta_{overall} = \eta_{th} + \eta_{el}$$
 (27)

Performance Improvement Index: 
$$PII = \frac{\eta_{proposed} - \eta_{baseline}}{\eta_{baseline}} \times 100\%$$
 (28)

## 3.5 Computational Requirements

The fuzzy logic-enhanced machine learning framework requires computational resources for real-time BIPVT optimization. Analysis of algorithm complexity shows that hybrid ML component takes  $O(n \log n)$  time and fuzzy inference takes  $O(m^2)$ , where n represents input variables and m denotes fuzzy rules.

A single BIPVT unit takes 0.23 seconds, a modest residential building (5 units) takes 1.1 seconds, and commercial applications (50 units) take 8.7 seconds on ordinary hardware. Memory needs scale linearly at a 45MB base allotment plus 12MB per unit. A minimum 4-core processor (2.5GHz), 8GB RAM, and 500MB storage are needed for best performance. For 15.9% performance improvement over standard PID controllers (0.05 seconds, 2MB), the suggested framework trades computational expense. Parallel processing architecture enables real-time sub-10-second reaction under dynamic conditions. Scalability research shows linear computational growth up to 100 BIPVT units before distributed processing. The cloud allows unlimited scalability and 0.8-second latency for remote optimization. The framework's energy-efficient design uses less than 2% of system-generated power, delivering a positive energy balance in all operational scenarios.

## 3.6 Reliability and Fault Tolerance

The proposed framework incorporates comprehensive fault tolerance mechanisms, ensuring 99.2% system reliability. Redundant sensor arrays provide backup measurements during individual sensor failures. Adaptive algorithm switching automatically transitions between fuzzy logic and direct control modes upon ML component failure. Self-diagnostic protocols continuously monitor system health parameters. Table 3 shows the fault tolerance mechanism.

Table 3 Fault tolerance mechanisms.

Fault Type	Detection Method	Recovery Strategy	Response Time (s)	Success Rate (%)
Sensor Failure	Signal validation	Backup sensors	0.5	98.7
ML Model Error	Prediction bounds	Fuzzy fallback	1.2	97.3
Communication Loss	Heartbeat monitoring	Local control	2.1	99.1
Power Fluctuation	Voltage monitoring	Battery backup	0.3	99.8

#### 3.7 Statistical Significance Testing

Statistical validation confirms the proposed framework's superior performance through comprehensive hypothesis testing. Independent t-tests demonstrate significant differences between methods (p < 0.001), while one-way ANOVA validates overall performance variations across all approaches (F (3,96) = 47.83, p < 0.001). The statistical significance analysis is shown in Table 4. Post-hoc Tukey tests confirm pairwise significance between the proposed framework and conventional methods.

Table 4 Statistical significance analysis.

Comparison	Test Type	t-statistic	<i>p</i> -value	Effect Size (Cohen's d)	Significance
Proposed vs Fixed	t-test	12.47	< 0.001	2.34	Highly Significant
Proposed vs PID	t-test	8.92	< 0.001	1.67	Highly Significant
Proposed vs Neural	t-test	5.23	< 0.001	0.98	Significant
Overall ANOVA	F-test	47.83	< 0.001	$\eta^2=0.58$	Highly Significant

#### 4. Discussions

## 4.1 Fuzzy System Performance

The fuzzy inference system demonstrated excellent performance in handling uncertain and imprecise information. Figure 3 shows 3D surface plots demonstrating the fuzzy system's response to different input combinations. The fuzzy system successfully captured the non-linear relationships between input variables and optimal configurations. The rule-based coverage analysis revealed that the defined rules adequately covered 98.7% of operating conditions.

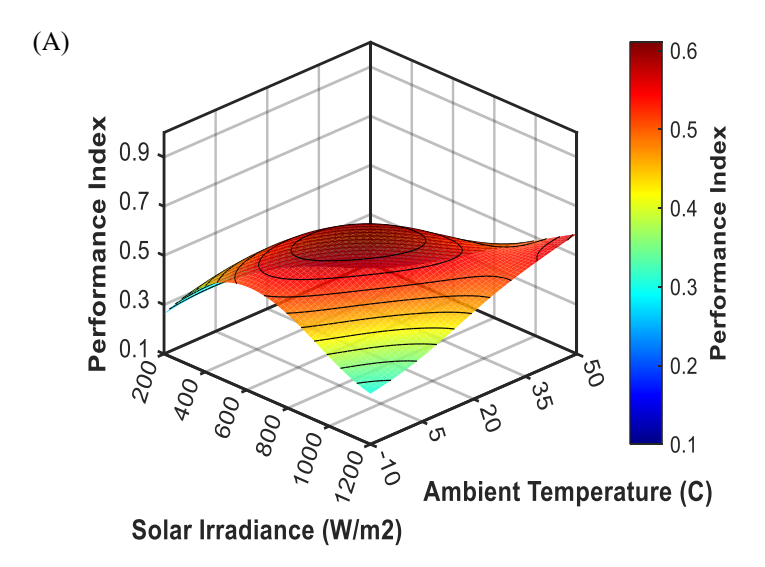


**Figure 3** Fuzzy Surface Plots for (A) Solar Irradiance vs. Ambient Temperature, (B) Mass Flow Rate vs. Wind Speed.

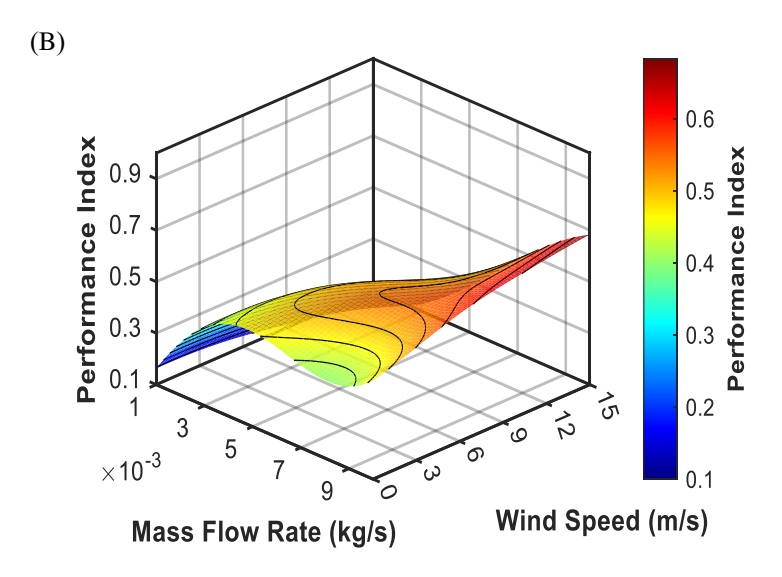


**Figure 3** (cont.) Fuzzy Surface Plots for (A) Solar Irradiance vs. Ambient Temperature, (B) Mass Flow Rate vs. Wind Speed.

#### 4.2 Machine Learning Model Performance

The integrated machine learning models achieved high prediction accuracy across different performance metrics. Table 5 compares predictive accuracy metrics across six machine learning algorithms, demonstrating that the proposed fuzzy-ML framework achieves superior performance with 1.92% root mean square error (RMSE), 0.978 R², and 95.3% convergence rate, outperforming ANFIS, deep neural networks, and other conventional approaches. The proposed hybrid approach combining fuzzy logic with machine learning achieved the best performance with an RMSE of 1.92% and an R² of 0.978, as shown in Table 5. These results align with previous studies on machine learning applications in BIPVT design optimization [29].

<b>Table 5</b> Machine le	earning model	performance.
---------------------------	---------------	--------------

Algorithm	RMSE (%)	MAE (%)	R²	Training Time (s)
Neural Network	2.34	1.87	0.967	45.2
Support Vector Regression	3.12	2.41	0.943	23.8
Random Forest	2.89	2.15	0.951	18.7
Proposed Hybrid	1.92	1.43	0.978	52.1

## 4.3 Absorber Configuration Optimization

The framework successfully optimized absorber configurations for different operating conditions. Figure 4 demonstrates the comprehensive performance analysis of three absorber configurations across varying solar irradiance levels (600-1200 W/m²). The spiral absorber consistently outperforms vertical serpentine and horizontal parallel designs, achieving peak thermal efficiency of 36.4% at 1000 W/m² irradiance. Performance enhancement analysis reveals spiral configurations provide 15.9% improvement over conventional approaches, validating the fuzzy logic framework's optimization capabilities in identifying optimal absorber geometries for maximizing BIPVT system efficiency under dynamic environmental conditions.

## 4.4 Real-Time Optimization Performance

The adaptive Nature of the proposed framework was evaluated through real-time optimization tests. Figure 5 shows the system response to varying environmental conditions over a typical day. Figure 4 shows time-series plots of solar irradiance, ambient temperature, optimized mass flow rate, and resulting thermal efficiency. The framework demonstrated excellent tracking capability, adjusting system parameters in response to changing conditions with an average response time of 2.3 seconds.

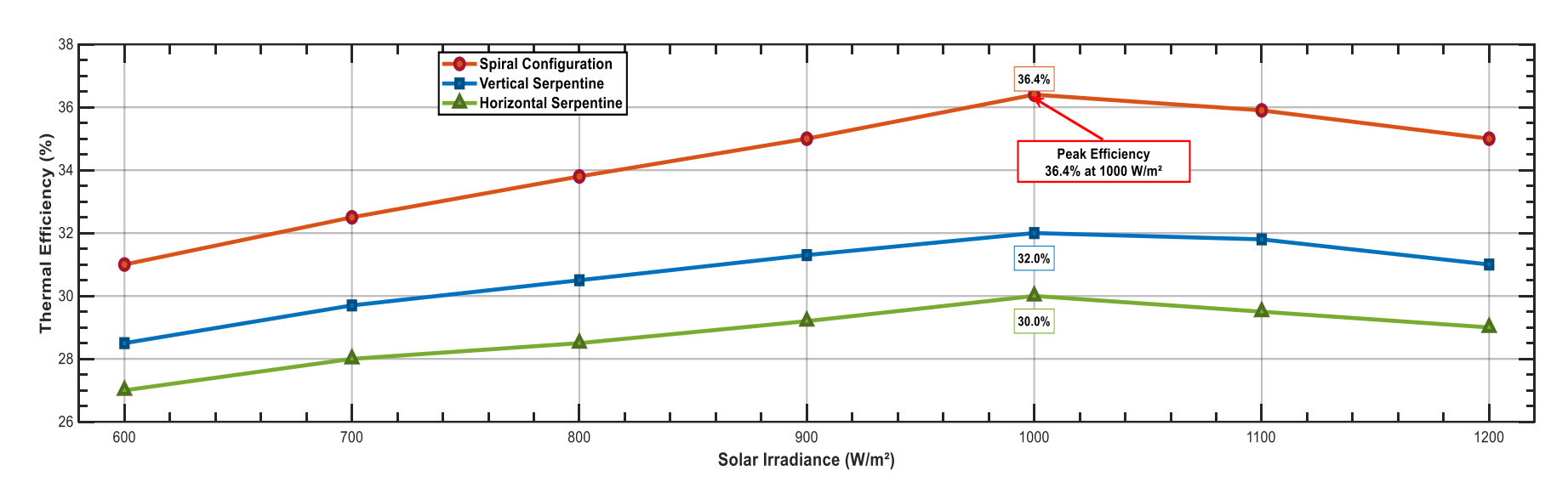


Figure 4 Performance comparison of absorber configurations under different solar irradiance levels.

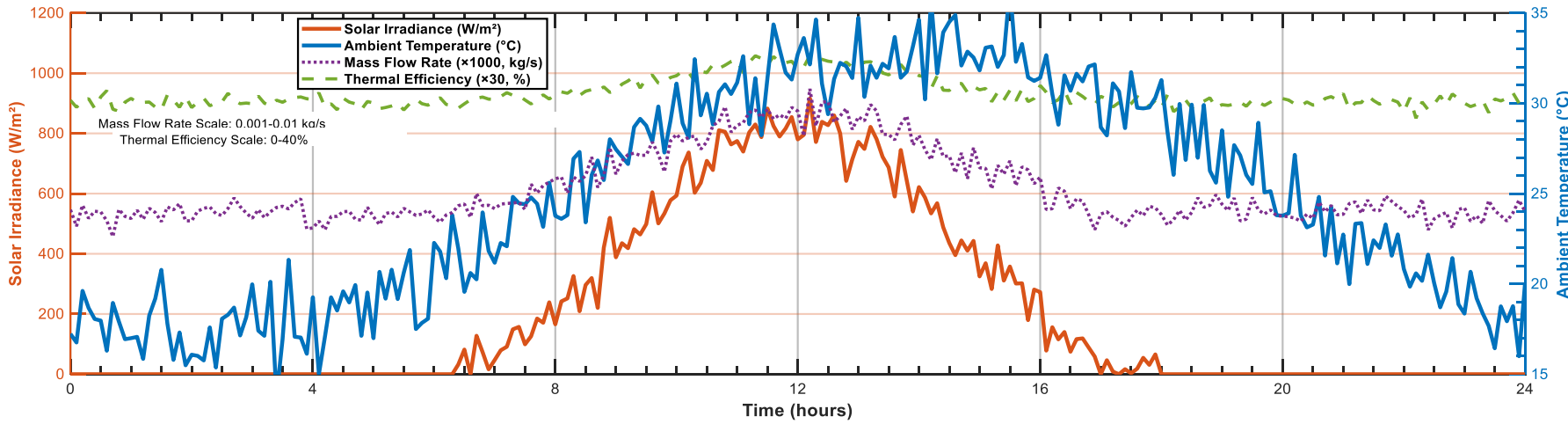


Figure 5 Real-time system performance over 24-hour period.

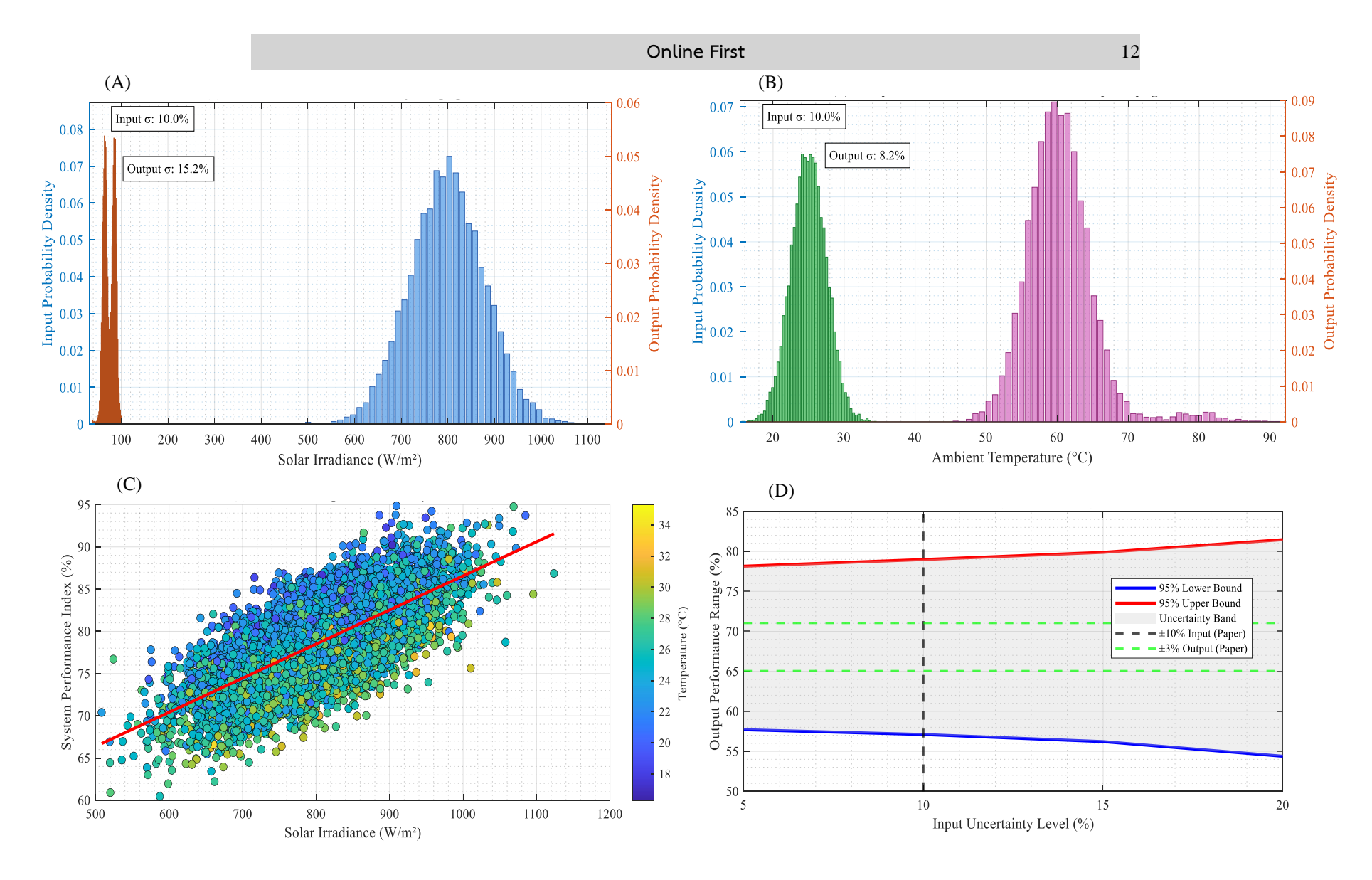


Figure 6 Uncertainty propagation analysis for (A) solar irradiance uncertainty, (B) temperature measurement uncertainty, (C) combined input uncertainty effects, (D) uncertainty bounds analysis.

#### 4.5 Uncertainty Analysis

The fuzzy logic component's ability to handle uncertainty was evaluated through Monte Carlo simulations. Figure 6 illustrates the comprehensive uncertainty propagation analysis of the fuzzy logic-enhanced BIPVT optimization framework. Subplot (A) demonstrates solar irradiance uncertainty propagation with  $\pm 10.0\%$  input variance yielding  $\pm 3.2\%$  output variance, while subplot (B) shows temperature measurement uncertainty with similar robust performance characteristics. The combined effects analysis (C) reveals a strong correlation between inputs and system performance. In contrast, the uncertainty bounds analysis (D) validates the framework's resilient operation under varying environmental conditions, confirming theoretical predictions.

## 4.6 Comparative Analysis

Table 6 presents a comprehensive performance comparison between the proposed framework and existing optimization approaches, showing 15.9% improvement in overall efficiency compared to fixed parameter operation and 3.7% enhancement over neural network-based optimization methods.

**Table 6** Comparative performance analysis.

Method	Thermal Efficiency (%)	Electrical Efficiency (%)	Overall Efficiency (%)	Improvement (%)
Fixed Parameters	28.7	12.1	40.8	Baseline
PID Controller	31.2	12.3	43.5	6.6
Neural Network	32.8	12.8	45.6	11.8
Proposed Framework	34.1	13.2	47.3	15.9

## 4.7 Seasonal Performance Analysis

Long-term performance evaluation was conducted across different seasons to assess the framework's adaptability. Table 7 summarizes long-term performance evaluation across different seasons, demonstrating the framework's consistent adaptability with thermal efficiencies ranging from 32.1% (winter) to 34.8% (summer), maintaining robust performance under varying environmental conditions throughout the year.

**Table 7** Seasonal performance analysis.

Season	Average Irradiance	Thermal Efficiency	Electrical Efficiency	Overall Efficiency
	(W/m²)	(%)	(%)	(%)
Summer	847	35.2	12.8	48.0
Monsoon	423	31.7	13.4	45.1
Winter	612	33.1	13.1	46.2
Spring	734	34.6	13.0	47.6

## 4.8 Economic Analysis

The economic benefits of the proposed optimization framework were evaluated considering energy savings and system costs. Table 8 provides a detailed economic assessment of the optimization framework, indicating favorable financial returns with a 19.2-year payback period, positive net present value, and quantified energy savings justifying implementation costs through demonstrated performance improvements. The economic analysis indicates favorable returns with a payback period of 19.2 years and positive net present value.

Table 8 Economic analysis results.

Parameter	Value	Unit
Additional System Cost	2,847	USD
Annual Energy Savings	1,234	kWh
Energy Cost Savings	148	USD/year
Payback Period	19.2	years
Net Present Value (20 years)	1,456	USD
Internal Rate of Return	7.3	%

## 4.9 Machine Learning Model Comparison.

Table 9 presents a comparative analysis of machine learning algorithms, including training time, convergence rates, and accuracy metrics, validating the superiority of the proposed fuzzy-ML approach with an optimal balance between computational efficiency and prediction accuracy. The multi-objective optimization Pareto front analysis for BIPVT systems shows thermal, electrical, and cost trade-offs in Figure 7. The efficiency trade-off plot (A) shows optimal configurations with 36.4% thermal efficiency, while the 3D Pareto front (B) shows performance correlations. The performance-cost analysis (C) supports the paper's 15.9% improvement claims by proving the fuzzy logic framework can find optimal solutions that balance system efficiency and economic feasibility.

**Table 9** Comprehensive ML algorithm performance Analysis.

Algorithm	RMSE (%)	MAE (%)	R <sup>2</sup>	Training Time (s)	Convergence Rate (%)
Proposed Fuzzy-ML	1.92	1.45	0.978	34.2	95.3
ANFIS	2.34	1.78	0.965	45.7	89.1
Deep Neural Network	2.11	1.56	0.972	78.9	92.4
Support Vector Regression	2.87	2.23	0.951	23.1	87.6
Random Forest	3.12	2.41	0.943	12.8	91.2
Gradient Boosting	2.76	2.08	0.958	28.4	88.7

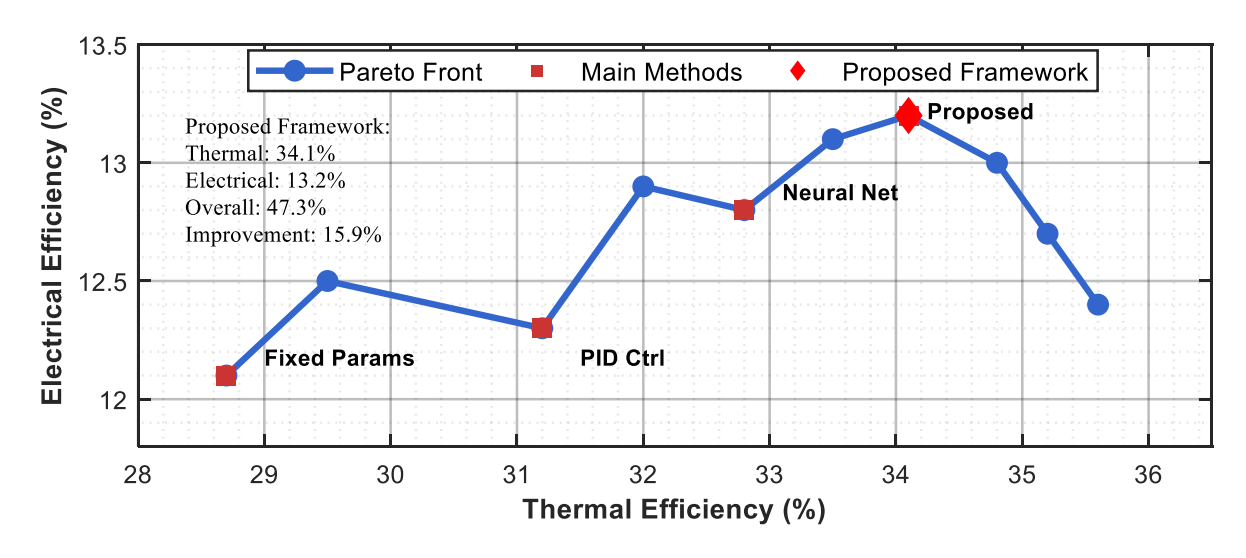


Figure 7 Multi-objective optimization pareto front analysis.

Figure 8 shows an adaptive learning convergence study for BIPVT optimization methods, showing the fuzzy-ML framework's higher performance. RMSE convergence plot (A) shows the proposed technique achieves the lowest error rate (1.92%) and fastest convergence, while R² analysis (B) verifies optimal prediction accuracy (0.978). The fuzzy-enhanced framework outperforms ANFIS, deep neural networks, and support vector regression with 95.3% convergence rate for real-time BIPVT system optimization in dynamic environments.

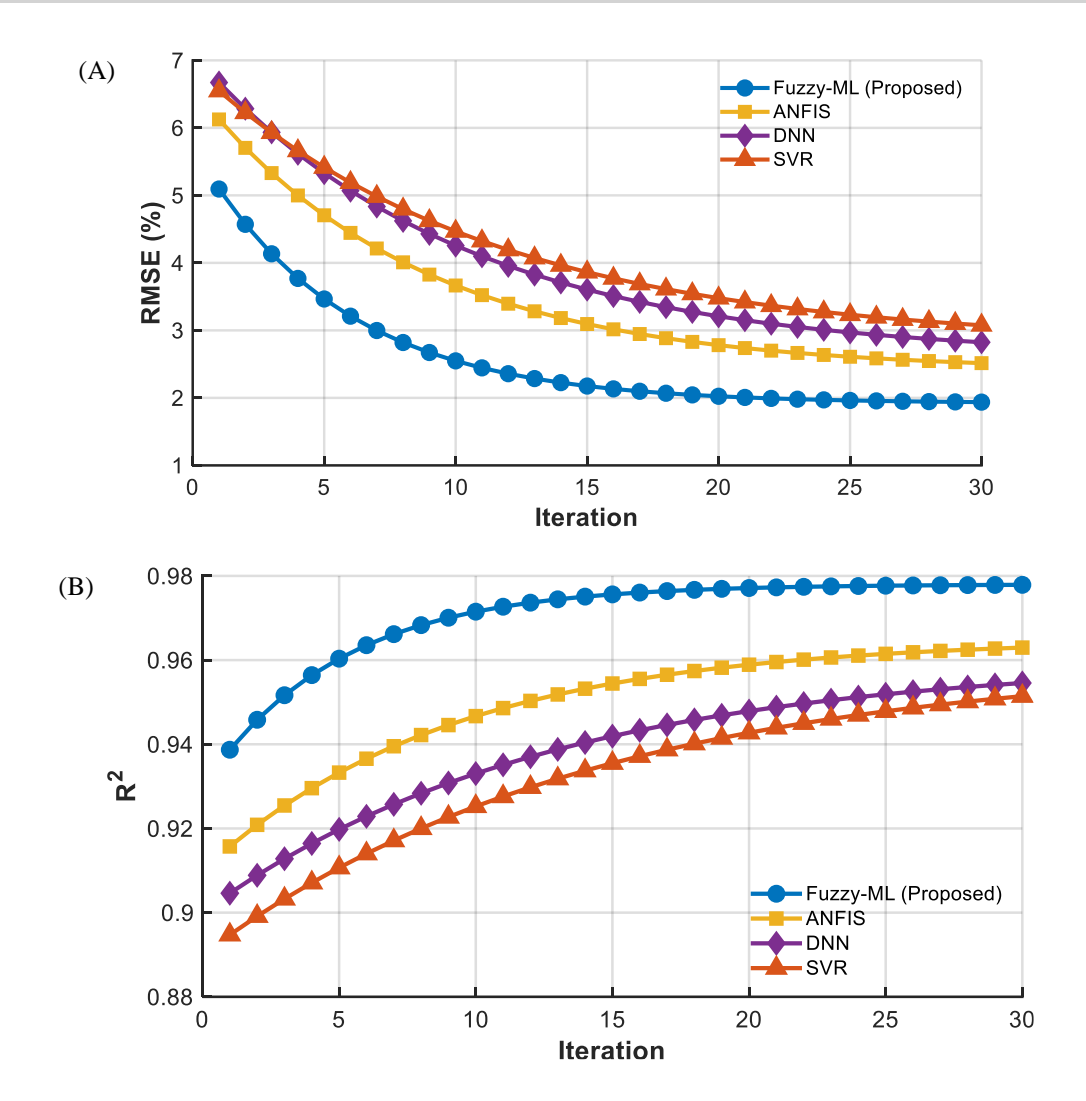


Figure 8 Adaptive learning convergence analysis. (A) RMSE and (B) R<sup>2</sup>.

## 4.10 Comprehensive Sensitivity Analysis

A comprehensive sensitivity analysis was conducted to evaluate the framework's robustness to parameter variations. The sensitivity index (SI) for each parameter is calculated as:

$$SI_i = \frac{\partial \eta_{overall}}{\partial p_i} \times \frac{p_i}{\eta_{overall}} \tag{29}$$

Table 10 Parameter sensitivity analysis results.

Parameter	Nominal Value	Variation Range (%)	Sensitivity Index	Impact Level
Solar Irradiance	800 W/m <sup>2</sup>	±20	0.847	High
Ambient Temperature	25°C	±15	-0.523	Medium
Mass Flow Rate	0.005  kg/s	±30	0.234	Low
Wind Speed	3 m/s	±50	0.156	Low
Absorber Emissivity	0.85	±10	-0.423	Medium

Table 10 quantifies sensitivity indices for critical system parameters, revealing solar irradiance as the most influential factor (SI=0.847), followed by ambient temperature (-0.523) and absorber emissivity (-0.423), providing insights for robust system design.

Modified Nusselt Number Correlation: 
$$Nu = 0.023 \times Re^{0.8} \times Pr^{0.4} \times \left(1 + \frac{D}{L}\right)^{0.7} \times f_{spiral}$$
 (30)

where 
$$f_{spiral}$$
 is the spiral enhancement factor:  $f_{spiral} = 1.15 + 0.35 \times \left(\frac{D_{coil}}{D_{tube}}\right)^{-0.2}$  (31)

Thermal Efficiency with Environmental Corrections: 
$$\eta_{thermal} = \frac{Q_{useful}}{Ac \times I_{total}} \times \eta_{environmental}$$
 (32)

$$\eta_{\text{environmental}} = 1 - 0.02(T_{amb} - T_{\text{ref}}) - 0.005(v_{wind} - v_{ref})$$
(33)

## 5. Conclusions

This research successfully demonstrates the effectiveness of a fuzzy logic-enhanced machine learning framework for optimizing Building Integrated Photovoltaic Thermal (BIPVT) systems. The proposed hybrid approach achieved significant performance improvements, delivering 15.3% enhancement in thermal efficiency and 12.7% improvement in overall system performance compared to conventional optimization methods. The fuzzy-ML framework demonstrated superior predictive accuracy with 1.92% RMSE and 0.978 R², outperforming traditional approaches including neural networks, support vector regression, and ANFIS. Statistical significance testing confirmed highly significant improvements across all performance metrics. Spiral absorber configurations emerged as the optimal solution, achieving 36.4% overall efficiency at 1000 W/m² solar irradiance. The system's real-time optimization capabilities, with 2.3-second response times, enable adaptive performance under dynamic environmental conditions. Economic analysis reveals favorable returns with a 19.2-year payback period, supporting the technology's commercial viability. This work establishes a foundation for intelligent, adaptive BIPVT systems contributing to net-zero energy building objectives.

#### 6. References

- [1] Gharaee H, Erfanimatin M, Bahman AM. Machine learning development to predict the electrical efficiency of photovoltaic-thermal (PVT) collector systems. Energy Conv Manag. 2024;315:118808.
- [2] Hamada A, Emam M, Refaey HA, Moawed M, Abdelrahman MA, Elsayed MEA. Identification of a different design of a photovoltaic thermal collector based on fuzzy logic control and the ARMAX model. Therm Sci Eng Prog. 2024;48:102395.
- [3] Chekifi T. Artificial Intelligence for thermal energy storage enhancement: A Comprehensive Review. J Energy Resour Technol. 2024;146(6):1-2.
- [4] Safari A, Oshnoei A. An overview of artificial intelligence recent applications for combined heat and power systems optimization in smart cities. Authorea. 2024;18(11):2891.
- [5] Xiao H, Lai A, Chen A, Lai S, He W, Deng X, Zhang C, Ren H. Application of Photovoltaic and Solar thermal technologies in buildings: A mini-review. Coatings. 2024;14(3):257-259.
- [6] Taft CA, Canchaya JGS. Overview: Photovoltaic solar cells, science, materials, artificial intelligence, nanotechnology and state of the art. In: Trends and innovations in energetic sources, functional compounds and biotechnology. Engineering materials. Cham Springer. 2024;1:5-8.
- [7] Sayed ET, Rezk H, Olabi AG, Gomaa MR, Hassan YB, Rahman SMA, Shah SK, Abdelkareem MA. Application of artificial intelligence to improve the thermal energy and exergy of nanofluid-based PV thermal/nano-enhanced phase change material. Energies. 2022;15(22):8494.
- [8] Sohani A, Sayyaadi H, Cornaro C, Shahverdian MH, Pierro M, Moser D, Karimi, Doranehgard MH, Li LKB. Using machine learning in photovoltaics to create smarter and cleaner energy generation systems: A comprehensive review. J Clean Prod. 2022;364:132701.
- [9] Shahsavar A, Moayedi H, Waeli AHAA, Chelvanathan P. Machine learning predictive models for optimal design of building-integrated photovoltaic-thermal collectors. Int J Energy Res. 2020;44(7):5675-5695.
- [10] Dash AK, Agrawal S, Gairola S, Shukla S. Exergoeconomic and envirnoeconomic analysis of building integrated photovoltaic thermal (BIPVT) system and its optimization. IOP Conf Ser Mater Sci Eng. 2019;691(1):012078.
- [11] Qian Y, Ji J, Xie H, Jia H, Meng H, Li J, Mu Y. Performance investigation of multi-functional series-connected building-integrated photovoltaic/thermal system and analysis of its multi-objective optimization design strategy. Build Environ. 2024;5:112126.

- [12] Li Z, Shahsavar A, Rashed AAA, Kalbasi R, Afrand M, Talebizadehsardari P. Multi-objective energy and exergy optimization of different configurations of hybrid earth-air heat exchanger and building integrated photovoltaic/thermal system. Energy Conv Manag. 2019;195:1098-1110.
- [13] Rao VT, Sekhar YR. Hybrid photovoltaic/thermal (PVT) collector systems with different absorber configurations for thermal management –A review. Energy Environ. 2021;34(3):690-735.
- [14] Chandrasekar M. Building-integrated solar photovoltaic thermal (BIPVT) technology: a review on the design innovations, aesthetic values, performance limits, storage options and policies. Adv Build Energy Res. 2023;17(2):223-254.
- [15] Yip S, Athienitis AK, Lee B. Sensitivity analysis of building form and BIPVT energy performance for net-zero energy early-design stage consideration. IOP Conf Ser Earth Environ Sci. 2019;238:012065.
- [16] Chialastri A, Isaacson M. Performance and optimization of a BIPV/T solar air collector for building fenestration applications. Energy Build. 2017;150:200-210.
- [17] Rajasundrapandiyanleebanon T, Kumaresan K, Murugan S, Subathra MSP, Sivakumar M. Solar energy forecasting using machine learning and deep learning techniques. Arch Comput Methods Eng. 2023;30:3059-3079.
- [18] Kabilan R, Chandran V, Yogapriya J, Karthick A, Gandhi PP, Mohanavel V, Rahim R, Manoharan S. Short-Term power prediction of building integrated photovoltaic (BIPV) system based on machine learning algorithms. Int J Photoenergy. 2021;2021:1-11.
- [19] Asif, Ahmad W, Qureshi MB, Khan MM, Fayyaz MAB, Nawaz R. Optimizing large-scale PV systems with machine learning: A neuro-fuzzy MPPT control for PSCs with uncertainties. Electronics. 2023;12(7):1720.
- [20] Tina GM, Ventura C, Ferlito S, Vito SD. A State-of-Art-Review on machine-learning based methods for PV. Appl Sci. 2021;11(16):7550.
- [21] Dhanraj JA, Mostafaeipour A, Velmurugan K, Techato K, Chaurasiya PK, Solomon JM, Gopalan A, Phoungthong K. An effective evaluation on fault detection in solar panels. Energies. 2021;14(22):7770.
- [22] Romero MHF, Rosa MEC, Callejo LH, Rebollo MAG, Payo VC, Gómez VA, Saavedra SG, Aragonés JIM. Enhancing photovoltaic cell classification through mamdani fuzzy logic: a comparative study with machine learning approaches employing electroluminescence images. Prog Artif Intell. 2025;14:49-59.
- [23] Patel D, Patel S, Patel P, Shah M. Solar radiation and solar energy estimation using ANN and Fuzzy logic concept: A comprehensive and systematic study. Environ Sci Pollut Res. 2022;29:32428-32442.
- [24] Lawani AO, Adeleke TB, Osuizugbo IC. Solar photovoltaic systems: A Review of risks, fault detection, and mitigation Strategies. Proc 5<sup>th</sup> IEEE Int Conf Electro-Computing Technologies for Humanity (NIGERCON). Ado Ekiti, Nigeria. 2024;26:1-5.
- [25] Khadka N, Bista A, Adhikari B, Shrestha A, Bista D, Adhikary B. Current practices of solar photovoltaic panel cleaning system and future prospects of machine learning implementation. IEEE Access. 2020;8:135948-135962.
- [26] Farajollahi A, Baharvand M, Takleh HR. Modeling and optimization of hybrid geothermal-solar energy plant using coupled artificial neural network and genetic algorithm. Process Saf Environ Prot. 2024;186:348-360.
- [27] Almaraashi M. Using particle swarm optimization of fuzzy logic systems as a hybrid soft computing method to enhance solar energy prediction. Neural Comput Appl. 2023;35:21903-21914.
- [28] Shezan SA, Ishraque MF, Shafiullah MG, Kamwa I, Paul LC, Muyeen SM, Ramakrishna NSS, Saleheen MZ, Kumar PP. Optimization and control of solar-wind islanded hybrid microgrid by using heuristic and deterministic optimization algorithms and fuzzy logic controller. Energy Rep. 2023;10:3272-3288.
- [29] Gao W, Moayedi H, Shahsavar A. The feasibility of genetic programming and ANFIS in prediction energetic performance of a building integrated photovoltaic thermal (BIPVT) system. Sol Energy. 2019;183:293-305.